Biomaterials Science

ROYAL SOCIETY OF CHEMISTRY

PAPER

View Article Online
View Journal | View Issue

Cite this: *Biomater. Sci.*, 2020, **8**, 3649

A microfluidics-derived growth factor gradient in a scaffold regulates stem cell activities for tendon-to-bone interface healing

Jingtong Lyu, †[a] Long Chen,†[b] Jiqiang Zhang,[c] Xia Kang,[a] Yunjiao Wang,[a] Wenjie Wu,[a] Hong Tang,[a] Jun Wu, *[d] Zhiyu He *[e] and Kanglai Tang*[a]

Treatment of tendon-to-bone interface injury has long been challenging in sports medicine. The major obstacle lies with the complicated three-layer structure of the tissue that consists of a bone region with osteocytes, a tendon region with tenocytes and a transitional region with chondrocytes. Conventional tissue engineering approaches using simply biomaterial scaffolds, stem cells and combinations of them had limited abilities to reconstruct the gradient structure with normal biomechanical properties. We herein aim to construct a three-layer structure with bone marrow-derived stem cells and tendon stem cells cultured in a decellularized tendon scaffold, through application of a gradient of biological cues in the longitudinal direction of the scaffold that guides the stem cells to differentiate and remodel the extracellular matrix in response to different medium concentrations in different regions. A microfluidic chip, on which a tree-like flow pattern was implemented, was adopted to create the concentration gradient in a dichotomous manner. We screened for an optimized seeding ratio between the two stem cell types before incubation of the scaffold in the medium concentration gradient and surgical implantation. Histology and immunohistochemistry assessments, both qualitatively and semi-quantitatively, showed that the microfluidic system provided desired guidance to the seeded stem cells that the healing at 8-week post-implantation presented a similar structure to that of a normal tendon-to-bone interface, which was outstanding compared to treatments without gradient guidance, stem cells or scaffolds where chaotic and fibrotic structures were obtained. This strategy offers a potentially translational tissue engineering approach for better outcomes in tendon-to-bone healing.

Received 12th February 2020,
Accepted 27th April 2020

DOI: 10.1039/d0bm00229a

rsc.li/biomaterials-science

Introduction

Rotator cuff tear, anterior cruciate ligament tear, and Achilles tendon tear are the three most common tendon injuries seen in sports medicine. In the United States, approximately 100 000 to 200 000 patients suffer from anterior cruciate ligament injury every year and the prevalence of symptomatic rotator cuff injuries range from 5% to 20%.[1] Meanwhile, the incidence of Achilles tendon ruptures was estimated to range from 5.5 to 9.9 per 100 000 people in North America.[2] Many of the cases involve injury to the tendon-to-bone interface and require surgeries. The aims of surgical repair are to reconstruct the anatomical structure and retrieve the mechanical performances of the tendon–bone interface that can bear the load from daily activities.[3] However, most of the currently adopted reconstruction surgery procedures, where direct linkage of the tendon and bone is performed, would result in fibrosis of the tendon-to-bone interface without normal biomechanical properties, giving rise to poor clinical outcomes and risks of tendon re-tearing. The fibrosis is caused by a lack of organized regeneration of the interface structure, a lack of cellularity, poor blood supply, *etc.*[4,5]

The tendon-to-bone interface has a gradient structure that is essential for its normal functions. It has a clear composition transition from the bone region, which is composed of type I collagen and minerals, to the tendon region, which is composed of well-aligned collagen I fibers, with an intermediate

[a]*Center of Sports Medicine of Orthopaedic Department, Southwest hospital, Third Military Medical University, Chongqing 400038, China. E-mail: Tangkanglai0001@hotmail.com*
[b]*Department of Orthopedics, Guizhou Provincial People's Hospital, Guiyang, Guizhou 550000, China*
[c]*Department of Neurology, Third Military Medical University, Chongqing 400038, China*
[d]*Key Laboratory of Sensing Technology and Biomedical Instrument of Guangdong Province, School of Engineering, Sun Yat-Sen University, Guangzhou, Guangdong 510006, China. E-mail: junwu1@mit.edu*
[e]*Key Laboratory of Marine Chemistry Theory and Technology, Ministry of Education, Ocean University of China, Qingdao 266100, China. E-mail: zhe19@jhu.edu*
†These authors contributed equally to this work.

transitional fibrocartilage region that contains both calcified collagen fibers connected to the bone region and non-calcified collagen fibers connected to the tendon region. The tendon region bears the tensile stress, while the bone region bears the load.[6] Due to the delicate, unique nature of the structures, tissue engineering approaches have been widely developed to promote tendon-to-bone interface healing.[7]

Traditional tissue engineering approaches for promoting tendon-to-bone interface healing usually involve scaffolds containing stem cells and/or growth factors.[8] Among all kinds of materials, biodegradable decellularized scaffolds are usually preferred due to their preserved extracellular matrix that mimics a favorable environment for cell differentiation and growth.[9,10] Pati *et al.* designed a tissue by bioprinting cell-laden constructs with a novel decellularized extracellular matrix (dECM); this tissue-engineered scaffold provided an optimized microenvironment conducive to the growth of three-dimensional structured tissue with high cell viability and functionality.[11] A. Shpichka *et al*. had also fabricated a 3D scaffold using two-photon polymerization, decellularization and cell encapsulation methods and the cell morphology, cytotoxicity and viability have been improved well.[12]

As for stem cells, bone marrow mesenchymal stem cells (BMSCs) have been shown to be a promising candidate due to their multipotency for differentiation into osteoblasts, chondroblasts, adipocytes, and tendon fibroblasts.[13–16] Another candidate is tendon stem cells (TSCs), as they present a strong promotive effect towards tendon regeneration.[17] The co-culture of both cell types was shown to be optimal for tendon repair,[18] and the osteogenic and tenogenic behaviors of the co-culture system could be regulated directly by the concentrations of the osteogenic medium.[19] Several previous works using a combination of scaffolds, stem cells and growth factors have shown its effectiveness in tendon-to-bone interface repair,[20–22] but it is still a major challenge to establish a microenvironment in the scaffold that can regulate the differentiation of seeded stem cells to form the gradient structure as in a normal tendon-to-bone interface. Although some success has been achieved to promote the formation of the desired composition transition by applying a growth factor concentration gradient through chemical conjugation,[5] only one growth factor (PDGF) was involved that might have rendered a suboptimal regulatory effect. Recently, there has been increasing interest in the presence of a concentration gradient focused on the microfluidic method. A microfluidic chip can establish the on-chip flow distribution and diffusion. Concentration gradients were formed by a distance of a few hundred micrometers and were generated in a series of microchannels.[23] K. Deekshith *et al*. designed a novel microfluidic chip and used a standard Y-shaped ladder design to obtain robust uniform chemical gradients.[24] F. Zheng *et al*. also achieved a microfluidic biochemical sensor with a cost-effective and rapid process which showed good sensitivity and a linear section at a low-level concentration of glucose (0–10 mM).[25]

Herein, we proposed to achieve a better tendon-to-bone composition transition in the scaffolds by regulating stem cell differentiation using a concentration gradient of the osteogenic induction medium containing multiple essential growth factors. A microfluidic chip, in which an implanted tree structure was designed and manufactured, was used to create the medium concentration gradient in a dichotomous manner by mixing the two introduced medium streams and their downstream mixtures sequentially. When the medium reaches the decellularized tendon scaffold seeded with bone marrow-derived stem cells (BMSCs) and tendon stem cells (TSCs), a total of eight concentrations are established longitudinally along the scaffold. We optimized the ratio between the stem cells for the best outcomes of the composition transition under the medium concentration gradient maintained by the microfluidic chip *in vitro* and implanted the scaffolds in a rat model of tendon tear injury to evaluate the effectiveness of tendon-to-bone repair. We demonstrate this method as a powerful approach to create scaffolds that can mimic the unique gradient structure of the tendon-to-bone interface and a potentially translational technique for patient treatment.

Experimental reagents and instruments

Preparation and characterization of microfluidic chips

Polydimethylsiloxane (PDMS) microfluidic chips and poly (methyl methacrylate) (PMMA) top/bottom shields were fabricated by Capital Bio Corporation (China) using the design shown in Scheme 1. To examine the feasibility of the generation of a concentration gradient and the stability of the concentration gradient, two streams of water containing a red dye and a green dye, respectively, were introduced into the two top inlets of the chip. The colors from the 8 outlets were observed and recorded over a period of 72 h.

Preparation and characterization of the decellularized scaffold

Frozen Achilles tendons (DaQing Biotechnology Co., Ltd, China) were thawed at room temperature and trimmed into cylindrical segments of 1 cm length. The tendon segments underwent repeating freeze–thaw cycles (1 min in liquid nitrogen followed by 5 min in saline solution at 37 °C) five times. Following three washes in phosphate-buffered saline (PBS) for 30 min each, the tendon segments were treated with nuclease solution containing 100 μg mL^{-1} RNase and 150 IU mL^{-1} DNase (Roche Diagnostics, USA) at 37 °C. Finally, the decellularized tendons were washed six times with 50 mL of PBS for 30 min each with shaking. DNA assay (Quant-IT™ PicoGreen® dsDNA assay kit, Thermo Fisher Scientific, USA) was adopted to detect any residual host DNA to evaluate decellularization. Mechanical tests were performed to evaluate the preservation of the mechanical properties of the decellularized scaffolds. For toxicity assessments, cells incubated with the medium in contact with the decellularized scaffold were subjected to cell apoptosis staining and flow cytometry (Annexin V-FITC/propidium iodide) to look for any abnormal increase of apoptotic behaviors. Scanning electron microscopy (SEM, ZEISS Gemini)

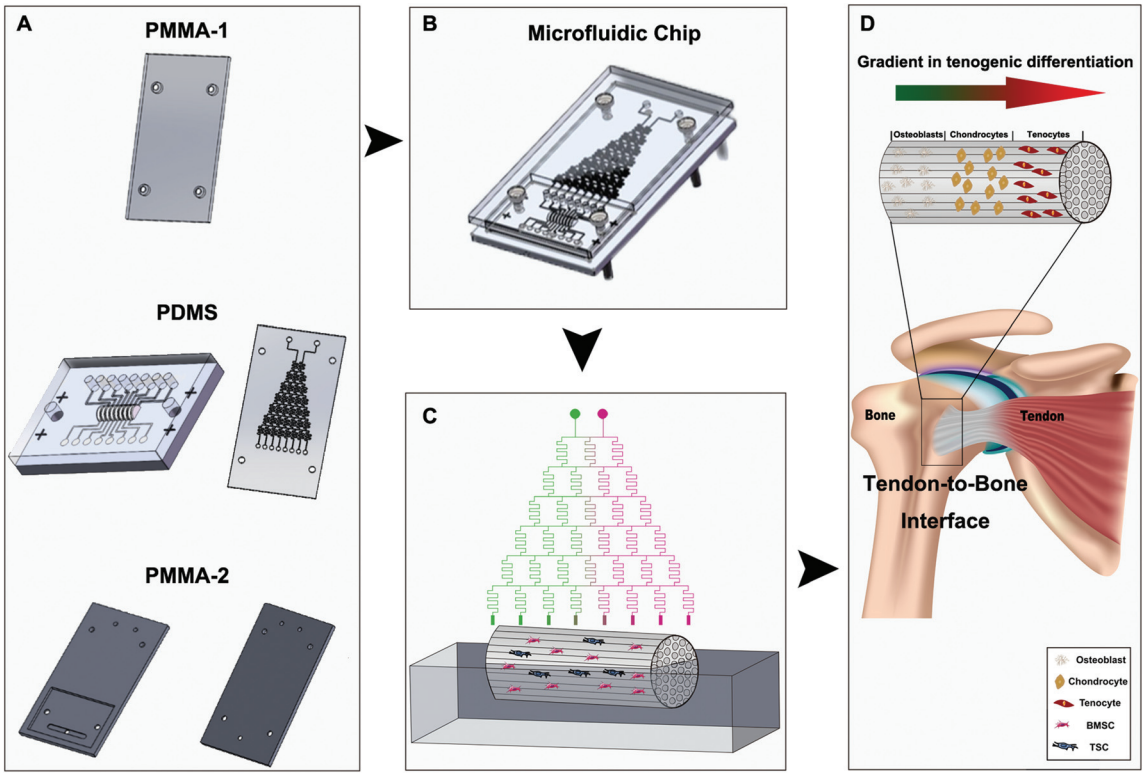

Scheme 1

was performed to observe the microstructures of the scaffold and to evaluate the stem cell attachment and ECM remodeling of the scaffold.

Isolation, co-culture, and identification of TSCs and BMSCs

TSCs were isolated and cultured as previously described.[26] Briefly, hind limb Achilles tendons were collected from euthanized rats and washed twice in PBS and digested in 3 mg mL^{-1} collagenase I (Sigma-Aldrich Co., Ltd, USA) and 4 mg mL^{-1} dispase (Sigma-Aldrich, USA) in PBS (pH 7.4) at 37 °C for 1 h. Undigested tissues were removed using a 200-mesh filter, and the resulting suspension was centrifuged at 600*g* for 5 min. The pelleted cells were resuspended in DMEM (Cyagen, China) supplemented with 10% fetal bovine serum (FBS) and cultured in a 35 mm dish coated with 0.1% gelatin. Bone marrow was obtained in accordance with the institutional review board approval from The Animal Research Ethics Committee of the Third Military Medical University, China. The bone marrow was isolated from the tibia and femur of eight-week-old male Sprague-Dawley (SD) rats. The bone marrow was added to DMEM with the medium refreshed every three days. After 10 days in culture, colonies of BMSCs and TSCs were formed. The BMSCs and TSCs were characterized by the cell markers of CD44(+), CD90(+), CD45(+), and CD34(−) for BMSCs and CD44(+), CD90(+), CD3(−), and CD34(−) for TSCs, respectively. To confirm the identification of the BMSCs and TSCs, the BMSCs were incubated with anti-CD44, CD90, CD34, and CD45 and the TSCs were incubated with anti-CD44, CD90, CD34, and CD3 for 1h, then incubated with Alexa Fluor594- and FITC-conjugated secondary antibodies for 30 min, and observed under a fluorescence microscope.

Quantitative reverse-transcription polymerase chain reaction (qRT-PCR)

Total RNA was isolated from the cells using Trizol (Invitrogen, USA). A First-Strand cDNA Synthesis kit (MBI Fermentas, USA) was used to synthesize the cDNA. The mRNA expression levels of ALP-L, TNC, SOX-9, and CEBP-α were determined with an ABI PRISM 7300 System (Applied Biosystems, Foster City, USA) using a Quant qRT-PCR (SYBR Green I) kit (Tiangen, China) according to the manufacturer's instructions. GAPDH was used as the endogenous control. Negative controls were included to identify any contamination. The primer sequences used in this research are listed in Table 1.

Surgical procedures

All animal procedures were performed in accordance with the Guidelines for Care and Use of Laboratory Animals of the Third Military Medical University and approved by the Animal Ethics Committee of the Third Military Medical University. Male SD rats (n = 32; 6–8 weeks old) were used for the study. For analgesia, chloral hydrate (0.1 mg kg^{-1}) was administered subcutaneously 30 min prior to surgery. In brief, the Achilles tendon of the right leg was exposed, and then grasped and sharply transected from its bone insertion to make a 1 cm defect. For repair using the scaffolds, a high-speed bur with a

Table 1 The sequences of the primers used for qRT-PCR

Gene	Forward primers	Reverse primers
TNC	5′-AAAGCAGCCACCCGCTATTA-3′	5′-TCAGGTTCTTTGGCTGTGGAG-3′
ALP-L	5′-GGCACCATGACTTCCCAGAA-3′	5′-CACCGTCCACCACCTTGTAA-3′
SOX-9	5′-GCCCCTTCAACCTTCCGCACTAC-3′	5′-CGGCTGCGTGGCTGTAGTAGGA-3′
CEBP-α	5′-GGTGGATAAGAACAGCAACG-3′	5′-GGTCATTGTCACTGGTCAAC-3′
GAPDH	5′-TGACTTCAACAGCAACTC-3′	5′-TGTAGCCATATTCATTGTCA-3′

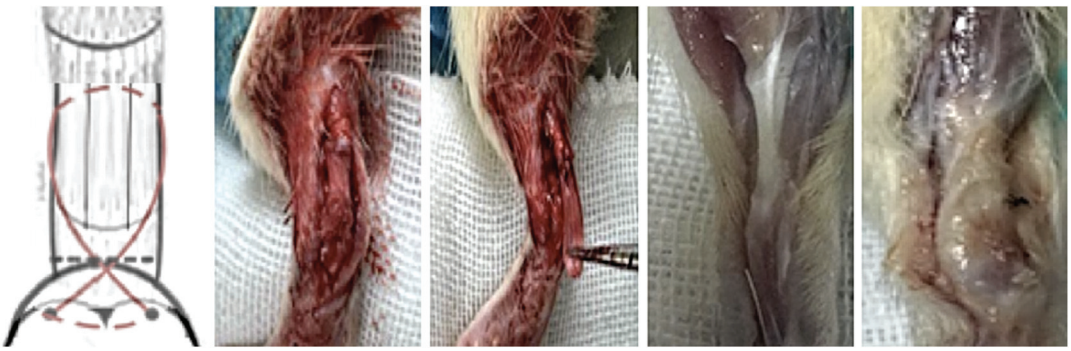

Fig. 1 The process of the operation of tendon-to-bone injury.

diameter of 2 mm was used to remove the remaining fibrocartilage from the footprint of the tendon insertion site. A 0.5 mm bone tunnel was drilled through the calcaneus. A suture was then passed through the bone tunnel and tied, securing the bone end of the scaffold to the footprint. Then the tendon end of the scaffold was sutured to the tendon (Fig. 1). The skin was closed with a 4-0 vicryl suture.

The rats were divided into four groups: the control group without treatment; the decellularized tendon scaffold group with implantation of the scaffold in the absence of stem cells; the decellularized tendon scaffold + cell group, for which the cell-seeded scaffold was directly implanted without culture in the chamber with control of medium supply by the microfluidic chip; and the microfluidic chip group, for which a 2-week culture in the chamber was followed after cell seeding before surgical implantation. After eight weeks, the rats were sacrificed and the bone–tendon area was collected and assessed by hematoxylin–eosin (H&E) staining, Masson's trichrome staining, and immunohistochemical staining.

H&E, Masson's trichrome, and immunohistochemical staining

The tendon–bone interface was harvested by slicing transversely at 1 cm proximal to the bone–tendon junction. Sections with 5 μm thickness were cut in the transverse plane and subjected to H&E or Masson's trichrome staining and microscopic observations. The cross-sections were also immunohistochemically stained for collagen type I (Col I), II (Col II), and III (Col III), SOX-9, and SCX. Deparaffinized cross-sections were incubated with proteinase K for antigen retrieval for 10 min, peroxidase blocking solution for 5 min, and 10% goat serum solution for 30 min. Then, the cross-sections were incubated with primary antibodies against Col I, Col II, Col III, SCX, and SOX-9 followed by peroxidase-labeled polymer-conjugated secondary antibodies. Finally, the cross-sections were incubated with 3,30-diaminobenzidine for 10 min to visualize the antibody binding.

We adopted a grading system to evaluate the efficacy of the treatments of different groups according to previous reports.[27] There are six major criteria: (1) collagen fiber continuity; (2) collagen fibers oriented in parallel; (3) collagen fiber density; (4) maturation of the tendon–bone interface structure; (5) vascularity; and (6) cellularity. The observations from tissue sections were evaluated and categorized into 4 levels from G0, which represents the poorest outcome, to G3, which represents the best outcome, as fully described in Table 2. A score of 1, 2, 3 and 4 was granted to G0, G1, G2 and G3, respectively, for statistical analysis.

Table 2 Histological grading criteria of the tendon-to-bone interface healing

Parameter	G0	G1	G2	G3
Collagen fiber continuity	25%	25–50%	50–75%	75%
Collagen fibers oriented in parallel	25%	25–50%	50–75%	75%
Collagen fiber density	Very loose	Loose	Dense	Very dense
Maturation of the tendon–bone interface structure	Poorly organized	Mildly organized	Moderately organized	Markedly organized
Vascularity	Minimally present	Mildly present	Moderately present	Markedly present
Cellularity	Minimally present	Mildly present	Moderately present	Markedly present

Statistical analyses

Data were analyzed using SPSS software (version 15.0; SPSS Inc.) and GraphPad Prism 7. A Mann–Whitney U test with a Bonferroni correction for multiple comparisons was performed to evaluate differences between groups for the histological data. One-way ANOVA was conducted for comparison between two groups for the mechanical and cell apoptosis tests. The results are presented as mean ± standard deviation, and significant differences were claimed with a $p < 0.05$.

Results and discussion

Manufacture and characterization of the microfluidic chip

The design of the 3D co-culture system is shown in Scheme 1, in which the decellularized scaffold seeded with BMSCs and TSCs was placed in a chamber, supplied with culture medium controlled by the microfluidic chip over the entire period of 2 weeks for the tissue formation. The key concept of the design is to generate a concentration gradient of the functional cytokines in the osteogenic induction medium (from none as in pure DMEM to full cytokine supply as in pure osteogenic induction medium), to promote the cultured stem cells in the scaffold to undergo cytokine-driven differentiation into different cell types to mimic the tendon-to-bone interface. In other words, the higher the concentration of the osteogenic induction medium, the more likely the BMSCs undergo differentiation into osteocytes; the more diluted the osteogenic induction medium, the more TSCs differentiate into tenocytes and the more the extracellular matrix (ECM) is regulated to have more aligned collagen fibers. Between these two regions, there is an intermediate level of the cytokines in the medium where both stem cells play a role in the tissue formation, forming a transition region.

The microfluidic chip comprises three layers (Fig. 2A and B). The chip was implemented into the intermediate 2 mm polydimethylsiloxane (PDMS) layer, where a tree-like microfluidic structure with a channel width of 200 μm was fabricated by etching. The chip was fixed and sealed by two layers of 5 mm poly(methyl methacrylate) (PMMA) shields. Pure osteogenic induction medium (medium concentration = 1) and pure DMEM (medium concentration = 0) enter the chip in two aligned channels on top of the chip and flow downstream, passing through many flow junctions. At each junction, one stream of the medium containing a higher concentration of osteogenic induction medium merges with the other stream with a lower concentration. Upon merging, the two streams are intensely mixed by the elongated channels before proceeding to the next flow junction. Each junction-channel part results in an averaged concentration of the medium out of the two emerging ones, thus creating an intermediate concentration. Multiple intermediate concentrations are therefore produced in a dichotomous manner. When reaching the culture chamber for the scaffold, a total of 6 intermediate concentrations are created between 0 and 1, thus rendering a concentration gradient inside the chamber (Fig. 2D).

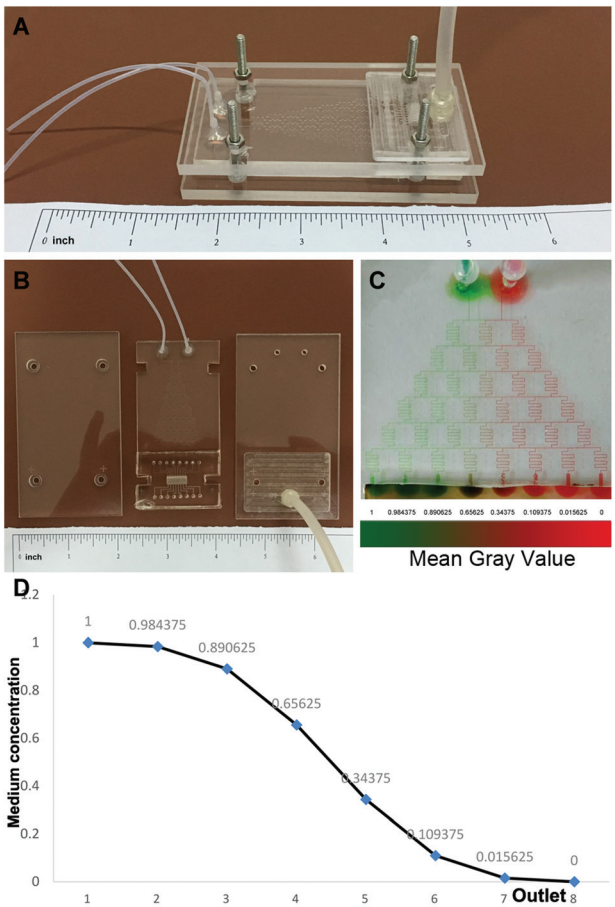

Fig. 2 Manufacture and characterization of the microfluidic chip. (A) The integral structure of the microfluidic chip; (B) the three layers of the microfluidic chip; (C) the tree-like flow pattern in the microfluidic chip for the generation of a concentration gradient, and illustration with two dyes with a red and a green color; and (D) the medium concentration gradient created in the culture chamber.

To validate, illustrate and examine the stability of the concentration gradient generated by the microfluidic chip, we applied streams with two miscible dyes into the system. 0.3 mm s^{-1} was adopted as the flow rate based on previous reports[28,29] to deliver sufficient nutrient supply to the cultured cells and at the same time minimize medium waste and potential shear effects on the cells. Establishment of a color gradient from pure green to pure red was observed (Fig. 2C), and the gradient was stable without perturbations over a period of 2 weeks. This ensured the consistency of the medium concentration in the cell culture experiments.

In addition to previous successful works on promoting the formation of a gradient structure in the tendon-to-bone interface by applying a gradient concentration of a single growth factor PDGF[5] or a concentration gradient of the mineral content also leading to a gradient of stiffness of the scaffolds,[30] we here provide a new strategy to take full advantage of the abilities of the stem cells to react to the concentration gradient of cytokines that allow modulations of the cell type and the ECM components in the scaffolds at the same

time. The transition from bone tissue to tendon tissue in the scaffold occurs simultaneously as a result of the controlled activities of the BMSCs and TSCs by the medium concentration gradient in full supply of the nutrients required for the growth of the tendon-to-bone interfaces. The concentration gradient is smooth and is formed in an extremely simple manner where only pure media need to be supplied into the system. Bio-microfluidic systems based on cells on scaffolds have been adapted for a variety of biomedical applications.[31,32] They are also cheap and scalable. Under steady flows of both media, the concentration gradient remains consistent as balanced convections and diffusions in the chamber for cell culture on the scaffold. This stability is believed to be essential for a consistent guidance to the stem cells.

Characterization of the decellularized scaffold

Full decellularization of the tendon tissue was characterized by the absence of DNA as observed by a fluorescence assay (Fig. 3A). The absence of DNA from the tissue donor indicated the absence of cells from the donor in the generated ECM of the scaffold, thus ensuring minimal immunogenicity upon implantation of the scaffolds. The decellularized scaffold maintained similar mechanical properties to the original tendon tissue, and for the maximum load, tensile strength and elongation at break tested, there was no statistically meaningful difference (Fig. 3B). This suggested that the ECM compositions and structures were well preserved in the decellularization process, and the decellularized scaffold was qualified for cell seeding.

The potential toxicity of the decellularized scaffold was assessed by the culture of TSCs in a medium pre-incubated with the scaffold for 24 hours. FITC fluorescence staining observations under a fluorescence microscope showed that the cells kept in such culture for 24 h, 48 h and 72 h showed no increasing population with early apoptosis (green) or progressing apoptosis (red) compared to the cells cultured without contact with the scaffold components (Fig. 4A). The results were confirmed by quantitative analysis through flow cytometry that the percentages of live and apoptotic cells are consistent between the two groups (Fig. 4B). Therefore, the scaffold was found to be suitable for subsequent cell cultures.

Scanning electron microscopy (SEM) was conducted to assess the microstructure of the scaffolds with and without seeded cells. The original tendon tissue presented a dense alignment of the collagen fibers, which was well preserved during the decellularization process as no major difference was observed afterwards (Fig. 5A). Upon seeding with BMSCs and TSCs, the cells grew on the scaffold and actively remodeled the ECM component to a less aligned structure (Fig. 5B). This indicated that the scaffold materials had an outstanding affinity to the stem cells that allowed adhesion and cell developments.

Decellularized scaffolds have several advantages, including the maintenance of the intrinsic tissue mechanical properties, inclusion of biological cues that are essential for cell proliferation, migration, and differentiation, good biocompatibility, moderate biodegradability, and low immunogenicity.[33] However, conventional methods to modify the decellularized scaffolds for cell culture purposes, such as chemical conjugation, physical adsorption,[22,34] *etc.*, are complicated and overall difficult, as accessibility of the whole scaffold, minimization of damage to the original ECM environment and characterization of the modifications can all be challenging. Our method in this study required no modification of the scaffolds, and the established gradient of the cytokines was robust due to free diffusion inside the scaffold. It was thus advantageous compared to the conventional methods.

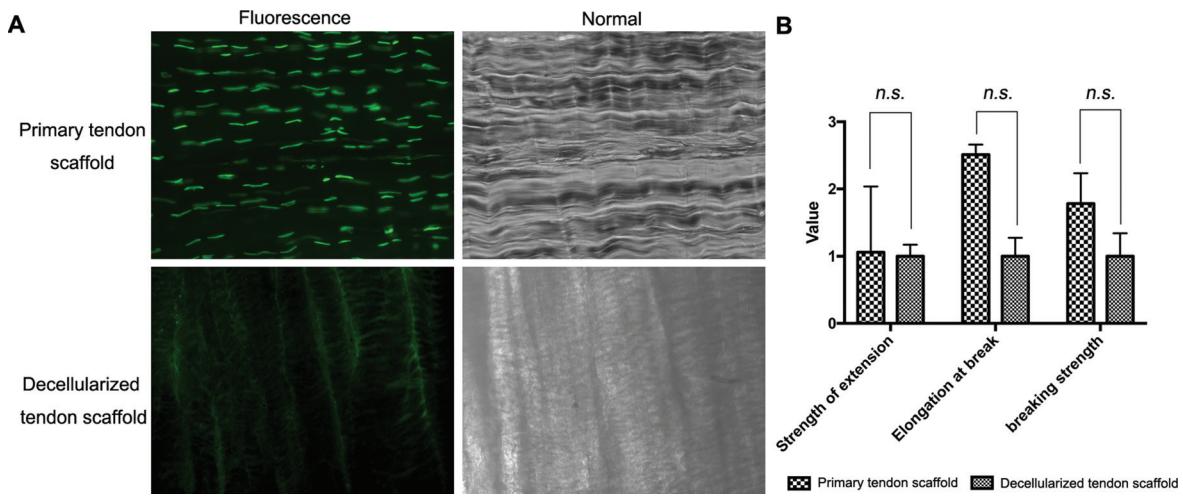

Fig. 3 Decellularization assessments of the tendon tissue and mechanical tests (n = 4, the primary tendon group: strength of extension was 4.875 ± 0.625, elongation at break was 2.043 ± 1.686, and the breaking strength was 0.414 ± 0.340. The decellularized tendon group: strength of extension was 6.223 ± 2.791, elongation at break was 0.979 ± 0.910, and the breaking strength was 0.453 ± 0.297. (A) DNA fluorescence assay that shows the absence of DNA in the tendon scaffold and (B) the maximum load, tensile strength and elongation at break tests of the original tendon tissue and decellularized scaffold. Scale bar = 200 μm.

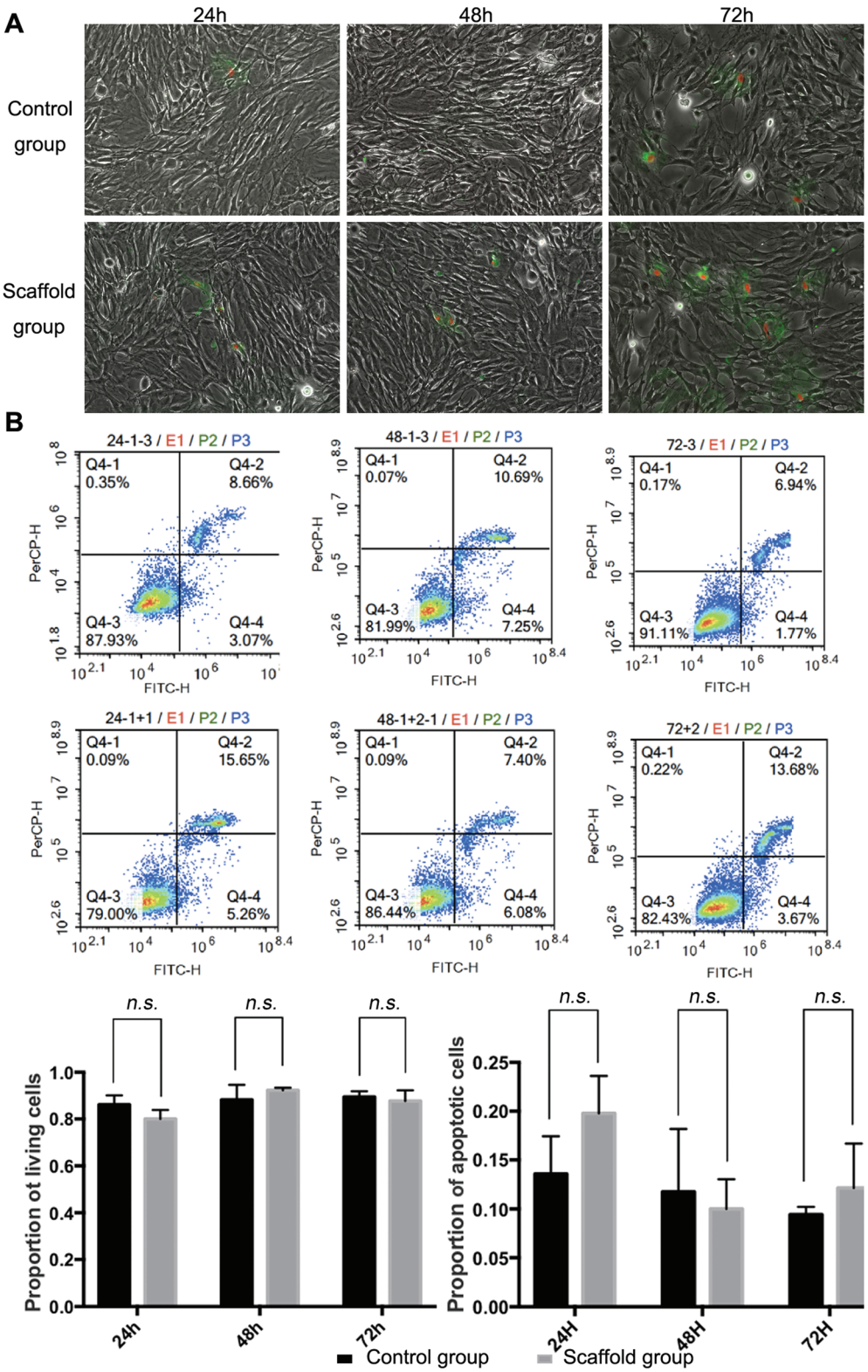

Fig. 4 Percentages of live and apoptotic cells. (A) FITC fluorescence staining observations using a fluorescence microscope and (B) the flow cytometry results showing the percentages of the live and apoptotic cells in the culture with or without coming into contact with the decellularized scaffold.

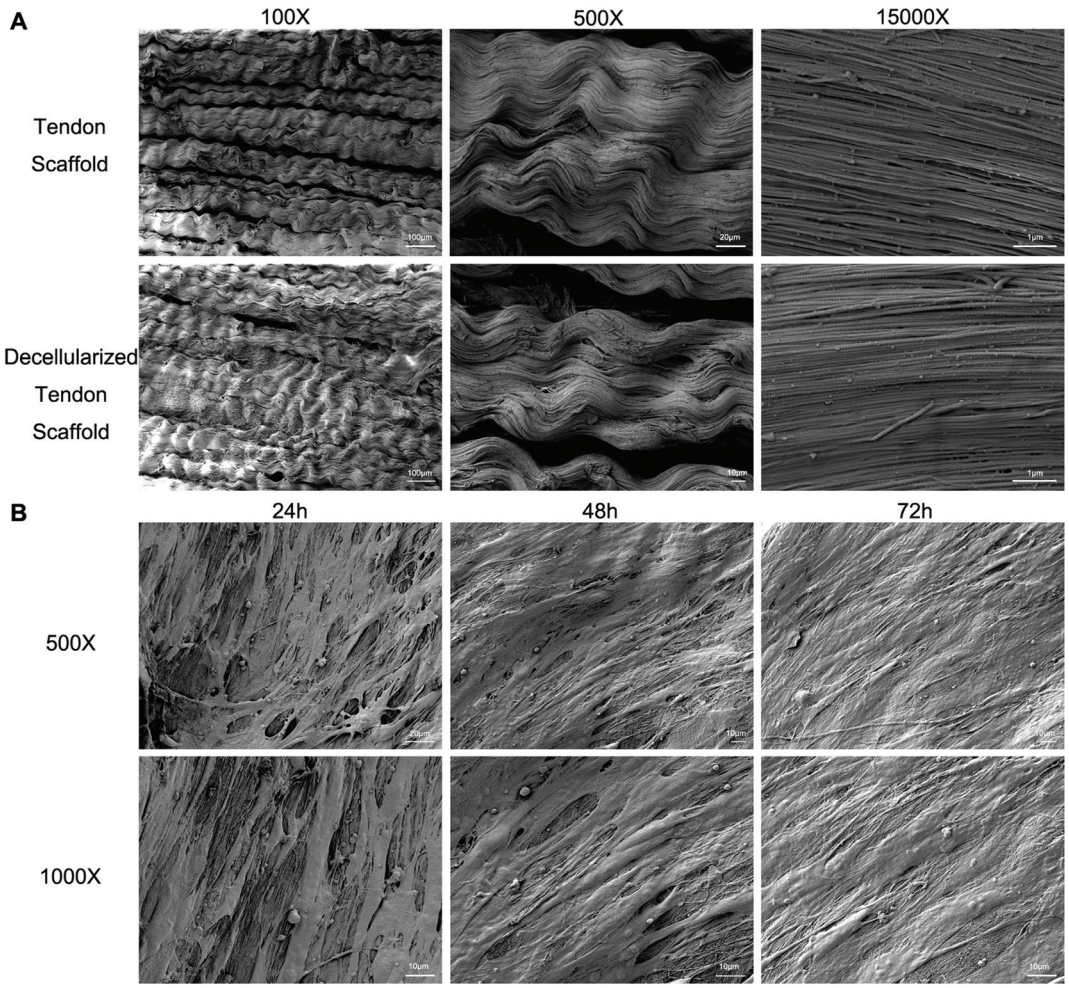

Fig. 5 Scanning electron microscopy (SEM) of the scaffold and cell adhesion. Representative SEM images of (A) the scaffold without cells seeded, scale bar = 100 μm in 100×, 20 μm in 200×, 1 μm in 15 000×; and (B) the scaffold with cells seeded, scale bar = 10 μm.

Isolation, identification, and co-culture cell ratio of TSCs and BMSCs

The BMSCs and TSCs were isolated according to previously reported methods (see the Experimental section). The extracted BMSCs exhibited a typical spindle-shaped appearance, while the TSCs presented a homogeneous population of a fibroblast-like appearance (Fig. 6A). To fully identify the stem cells, specific cell markers of the two cell types were examined. The cell markers specific to mesenchymal stem cells (MSCs), CD44 and CD90, were positive for both cell types. For BMSCs, the expression of CD45 (leukocyte common antigen) was low and the expression of CD34 (hematopoietic stem cell and progenitor cell marker) was negative, which proved that the BMSCs did not originate from the blood. For TSCs, the expression of both CD3 and CD34 was negative, suggesting that the TSCs derived were MSCs rather than blood-circulating stem cells, which were desired for downstream experiments.

The ratio between the BMSCs and TSCs in the co-culture system was screened in terms of the ability of the cultured stem cells to differentiate into tenocytes, osteocytes and chondrocytes, for which RT-qPCR was conducted to evaluate the mRNA expression level of the relevant genes of each cell type (TNC, ALP-L and SOX-9, respectively). For an ideal co-culture ratio, all three levels need to be high. At the same time, the stem cell co-culture should have a minimum adipogenesis tendency that may negatively affect the tensile strength of the formed tendon-to-bone interface, for which a key regulator in the process CEBP-α was assessed. Based on the aforementioned criteria, a culture ratio of BMSC : TSC = 1 : 2 was found to be optimal out of seven ratios tested, with a high level of tenogenesis ability, a moderate level of osteogenesis ability, a high level of chondrogenesis ability, and a low level of adipogenesis ability (Fig. 6B). This ratio was adopted to be tested in the animal model.

Most previous studies on using stem cells to promote the repair of the tendon-to-bone interface relied on a single stem cell type of BMSCs.[35–38] The important role of TSCs in tenogenesis was not discovered until recent findings showed that TSCs were found in tendon tissue that can differentiate into chondrocytes, osteocytes, and adipocytes, thus being a

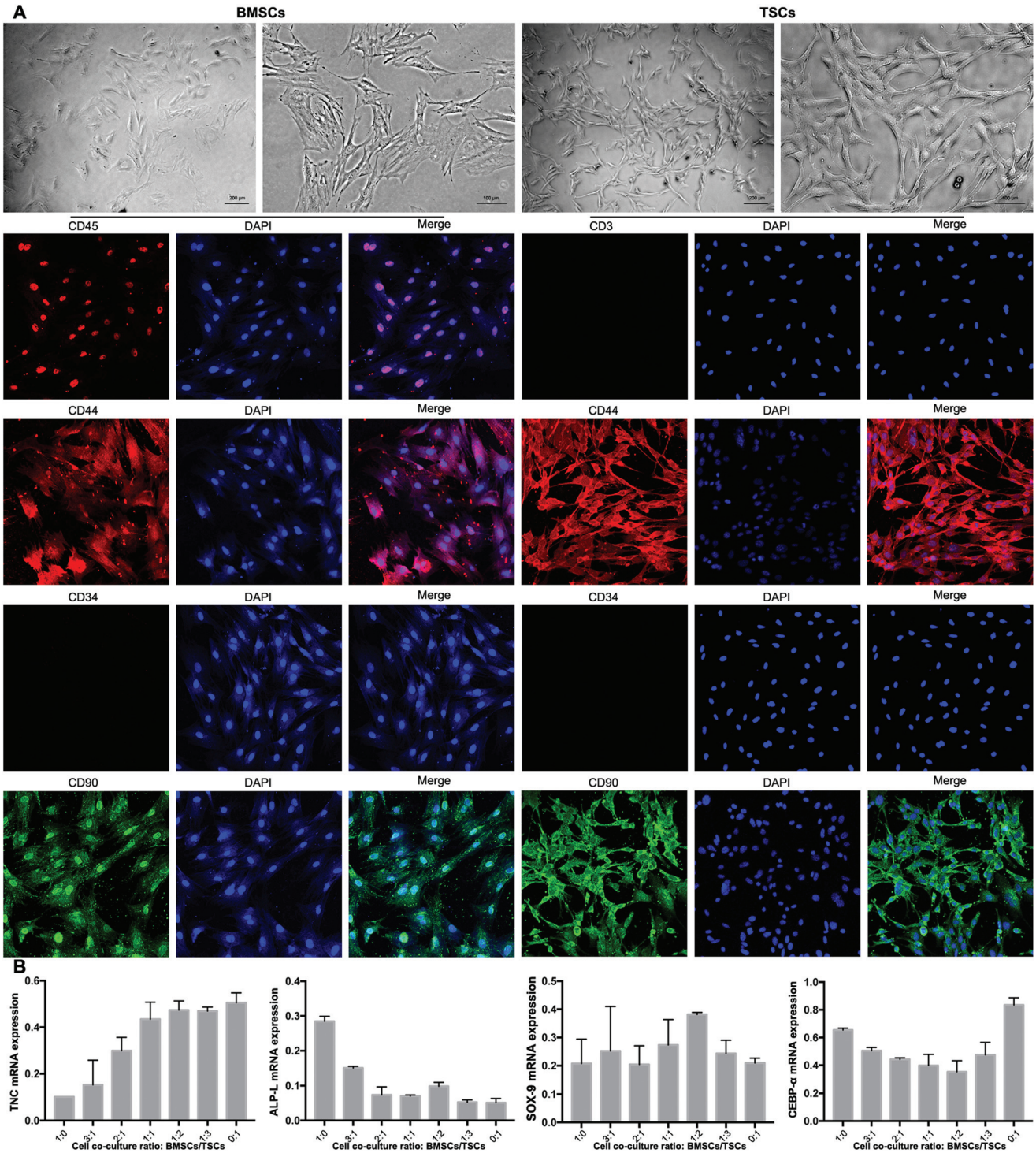

Fig. 6 The morphology and characteristics of bone marrow-derived stem cells (BMSCs) and tendon stem cells (TSCs), and mRNA expression (TNC, ALP-L, SOX-9 and CEBP-α) for BMSCs/TSCs in co-culture with different cell ratios. (A) The morphology (scale bar = 200 μm in lanes 1 and 3 and 100 μm in lanes 2 and 4) and cell markers of BMSCs and TSCs and (B) mRNA expression of TNC, ALP-L, SOX-9 and CEBP-α for BMSCs/TSCs in co-culture with different cell ratios (n = 3).

promising candidate stem cell type for tendon repair.[39–41] Our approach of a co-culture system takes advantage of the potential of both types of stem cells that would maximize the possibility of a positive outcome. Besides, the activities of the stem cells in the co-culture were regulated by the concentration gradient of the osteogenic induction medium controlled by the microfluidic chip. The stem cells adopted and the strategy to control their lineage commitment are preferen-

tially promising for repairing a complicated structure in a simple manner.

In vivo study

A total of 1×10^6 cells were seeded into the scaffold with a cell ratio of BMSC : TSC of 1 : 2. The scaffold was placed in the incubation chamber of the device with a concentration gradient of the osteogenic induction medium across the longitudinal direction of the scaffold as controlled by the microfluidic chip. The incubation with the concentration gradient was maintained for 2 weeks until surgical implantation. Histology assessments (H&E and Masson's trichrome) at an 8-week post-procedure time point were performed to evaluate the repair efficacy of the tendon-to-bone interface. In Fig. 7, the normal tendon-to-bone interface shows a typical three-layer structure with clear distinctions of bone tissue, tendon tissue and cartilage tissue in between. The control group showed a poor healing status at week 8 with the formation of massive fibrous tissue in the defect area. There was no smooth transition from the tendon tissue to the bone tissue, which resulted in poor prognosis for the normal function of the tendon-to-bone interface. The appreciable presence of inflammatory cells also indicated an unfavorable environment for normal tissue formation. The group implanted with a decellularized tendon scaffold group without any cells seeded showed improvement in the healing process as shown by cell growth and angiogenesis. However, the scaffold region had no order of the cell types that there was still not a clear distinction of different regions of a normal tendon-to-bone interface. Compared to the scaffold group, seeding of the stem cells in a plain culture medium (DMEM) did not result in an appreciable improvement of cell growth or tissue organization. This suggests that without proper guidance through biological cues, the stem cells cannot effectively differentiate into the desired cell types

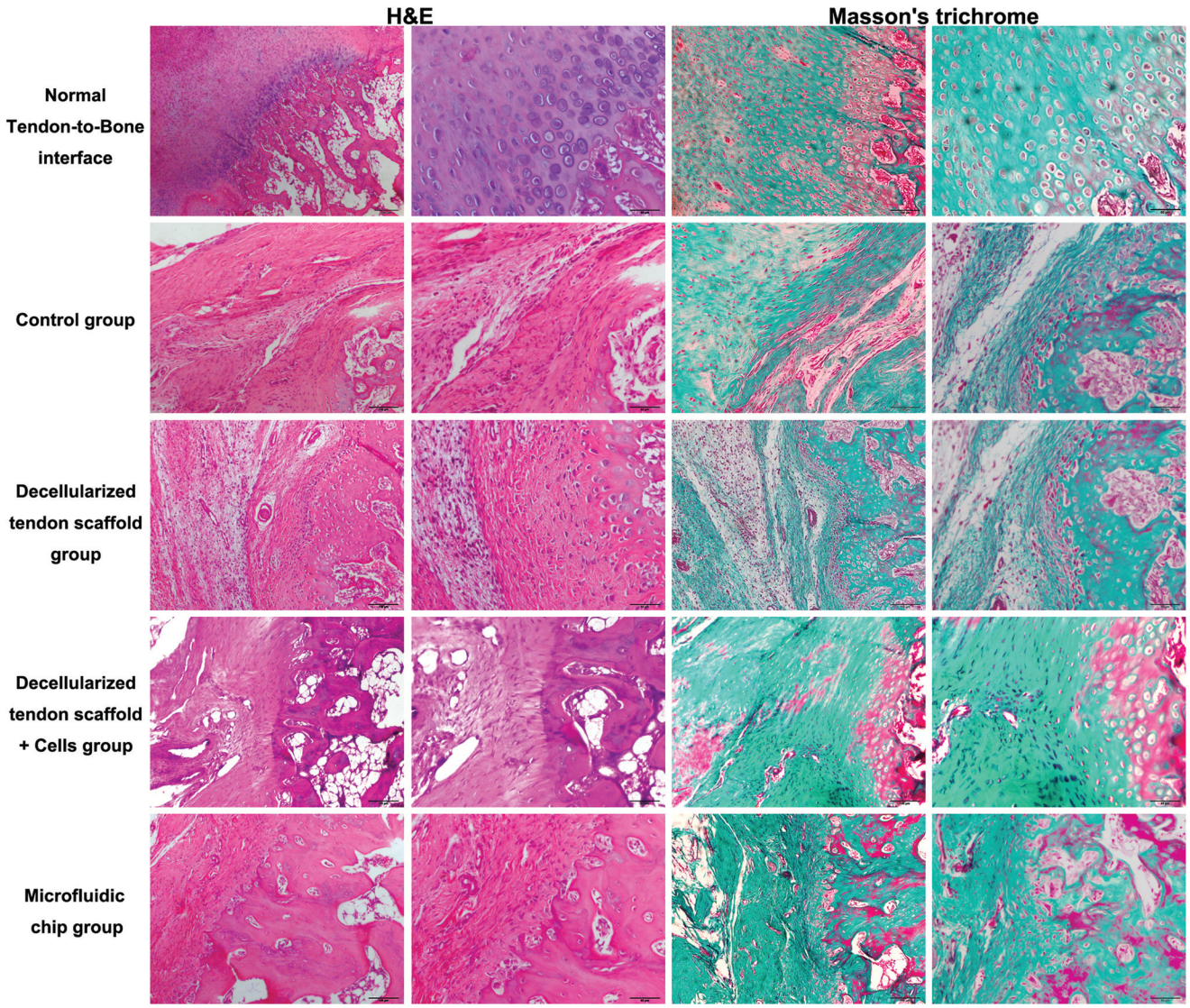

Fig. 7 H&E and Masson's trichrome staining of the tendon-to-bone interface at 8-week post-implantation. Scale bar = 100 μm in lanes 1 and 3 and 50 μm in lanes 2 and 4.

or actively remodel the ECM compositions and structures. This was addressed by the microfluidic chip, as seen in the microfluidic chip group, and the tendon-to-bone interface in the scaffold region showed a similar 3-layer structure to the normal tissue when the stem cells were subjected to the concentration gradient of the culture medium. With a high concentration of the osteogenic induction medium on one end, the stem cell co-culture favored an osteogenic development, while on the other end tendon tissue was formed. In the middle region where the concentration of the osteogenic induction medium was intermediate, chondrocytes were generated forming a transitional region connecting the two on each end. Angiogenesis could also be well appreciated, indicating good efficacy of the healing process. The effectiveness of the established medium concentration gradient on the formation of the gradient structure of the tendon-to-bone interface was remarkable.

Immunohistochemistry assessments were also performed to compare the efficacy of different groups (Fig. 8). There was no major difference in the deposition of collagen I, collagen II or collagen III among the experimental groups. For the chondrogenesis indicator SOX-9, the microfluidic chip group showed significantly more expression than the other groups, indicating a better formation of the transitional region in the tendon-to-bone interface. This was considered as major evidence of the three-layer structure desired for tendon-to-bone interface repair by concentration gradient-regulated stem cell activities in the scaffold. For the tendon tissue indicator SCX, there was no difference among the groups in terms of the levels of expression. However, the microfluidic chip group showed some degree of alignment of the tendon tissue, indicating better reconstruction of the tendon region. The results were coherent with the histology assessments that the microfluidic system benefited the treatment by co-culture of stem cells on a decellularized scaffold.

The full set of evaluation results according to the grading system is summarized in Table 3, showing the distribution of the 8 animals in each group into the 4 evaluation levels. Fig. 9

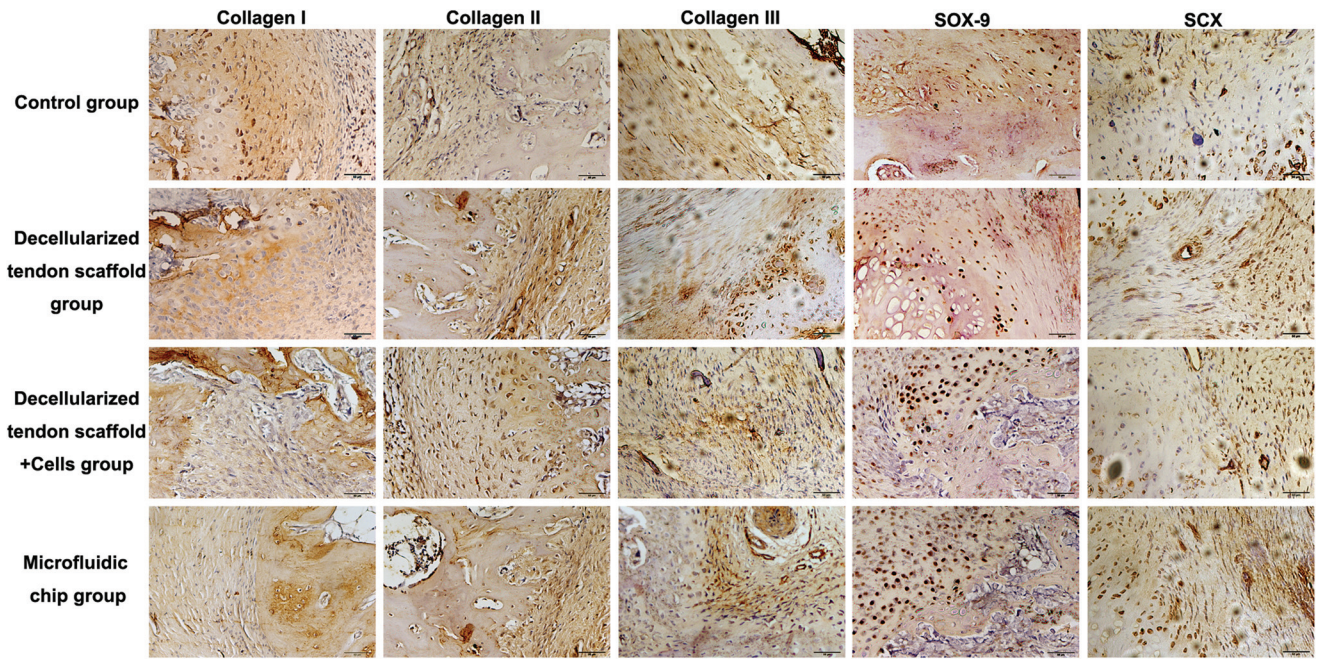

Fig. 8 Collagen I, collagen II, collagen III, SOX-9 and SCX immunohistochemical staining of the tendon-to-bone interface at 8-week post-implantation. Scale bar = 50 μm.

Table 3 The evaluation results for each group according to the histological grading criteria

	Control group (n = 8)				Decellularized tendon scaffold group (n = 8)				Decellularized tendon scaffold + cell group (n = 8)				Microfluidic chip group (n = 8)			
Item	G0	G1	G2	G3	G0	G1	G2	G3	G0	G1	G2	G3	G0	G1	G2	G3
Collagen fiber continuity	8	0	0	0	2	3	1	2	0	2	4	2	0	1	2	5
Collagen fibers oriented in parallel	8	0	0	0	8	0	0	0	6	2	0	0	2	2	3	1
Collagen fiber density	8	0	0	0	0	1	5	2	0	1	5	2	0	0	3	5
Maturation of the tendon-to-bone interface structure	8	0	0	0	6	1	1	0	5	2	1	0	2	2	1	3
Vascularity	3	3	1	1	3	2	2	1	2	2	2	2	0	2	3	3
Cellularity	3	5	0	0	3	4	1	0	0	1	4	3	0	0	3	5

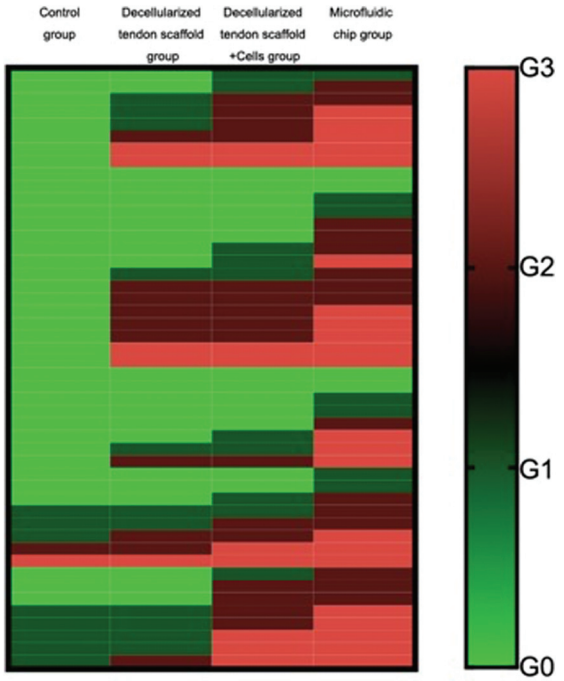

Fig. 9 Histological grading distribution for each group. G0, G1, G2 and G3 (corresponding to grades of 1, 2, 3 and 4, respectively) are reflected in the figure from green to red. Each row represents a single criterion of a single animal within the group. The group that received an overall grading distribution with more red illustrations had a better overall efficacy for the tendon-to-bone interface healing.

shows an overall view of the evaluation results for each group, with each evaluation criterion of each animal illustrated as a separate row. This suggests that the microfluidic group had the best average outcome among all the other groups for the repair of the tendon-to-bone interface.

To validate the conclusion, the Mann–Whitney *U* test was performed between groups to achieve statistical significance ($p < 0.05$), and the results are shown in Table 4. Briefly, as for the collagen fiber continuity and collagen fiber density, the increasing mean from the control group, the decellularized tendon scaffold group, and the decellularized tendon scaffold + cell group to the microfluidic chip group and the statistical significance between any two of the groups (with only one non-important exception of 0.167) suggest that the involvement of scaffolds, stem cells, and the concentration gradient for guidance of the stem cells is favorable towards better healing of the tendon-to-bone interface. As for collagen fibers oriented in parallel, maturation of the tendon-to-bone interface structure and vascularity, the microfluidic chip group stood out with the best outcome due to the significant difference compared to any of the other groups. As for cellularity, the decellularized tendon scaffold + cell group and the microfluidic chip group had similar levels of the best outcome that was incomparable with the other two groups, suggesting that the stem cells played a vital role in cell growth during the repair of the tendon-to-bone interface. In conclusion, the microfluidic chip design greatly improved the treatment

Table 4 The results of the Mann–Whitney *U* test for histological scores between groups

Parameter	Control group	Decellularized tendon scaffold group	Decellularized tendon scaffold + cell group	Microfluidic chip group
Collagen fiber continuity				
Group A		0.002	<0.001	<0.001
Group B			0.047	0.011
Group C				0.039
Group D				
Collagen fibers oriented in parallel				
Group A		0.167	0.074	0.002
Group B			0.074	0.002
Group C				0.006
Group D				
Collagen fiber density				
Group A		<0.001	<0.001	<0.001
Group B			0.167	0.027
Group C				0.027
Group D				
Maturation of the tendon-to-bone interface structure				
Group A		0.074	0.039	0.002
Group B			0.120	0.008
Group C				0.014
Group D				
Vascularity				
Group A		0.146	0.074	0.008
Group B			0.096	0.014
Group C				<0.001
Group D				
Cellularity				
Group A		0.133	<0.001	<0.001
Group B			0.001	<0.001
Group C				0.055
Group D				

outcome from stem cells seeded on the decellularized scaffolds.

Conclusions

In this study, we successfully used a microfluidic chip to generate a concentration gradient of the osteogenic induction medium, thus a concentration gradient of the essential osteogenic growth factors, in a chamber where a decellularized tendon scaffold pre-seeded with BMSCs and TSCs was incubated. The stem cells seeded perform differentiation into different cell types, remodelling of the ECM compositions and structures, and regulation of cell growth differently in different regions of the scaffold in response to the concentration gradient, which form a three-layer structure in the scaffold consisting of a bone region with osteocytes, a tendon region with tenocytes and a transitional region with chondrocytes. The structure remarkably represented the complicated structure in the normal tendon-to-bone interface, as assessed by histology and immunohistochemistry assessments. A grading system was also adopted and it revealed that the stem cell-scaffold incubated with the concentration gradient in the microfluidic system had the best repair outcome in a tendon defect rat model. The strategy to generate the concentration gradient is advantageous in terms of the involvement of multiple essential growth factors as supplied in the functional medium and the ease of operation; thus it is believed to be a potential translational tissue engineering approach for the repair of the tendon-to-bone interface. Further directions will include investigations of the molecular pathways involved in the healing process guided by the microfluidic system, scale-up production of the scaffolds and *in vivo* functional studies after repair.

Conflicts of interest

There are no conflicts to declare.

Acknowledgements

This project was supported by the National Natural Science Foundation of China (Grant No. 8157090393), the Clinical Medical Research Personnel Training Program of Third Military University (Grant No. 2018XLC3009), the Doctoral Fund of Guizhou Provincial People's Hospital (Grant No. GZSYBS[2017] 04) and the Scientific and Technological Research Project for Traditional Chinese Medicine and Folk Medicine of Guizhou Provincial Administration of Traditional Chinese Medicine (Grant No. QZYY-2018-003).

References

1 K. Atesok, F. H. Fu, M. R. Wolf, M. Ochi, L. M. Jazrawi, M. N. Doral, J. H. Lubowitz and S. A. Rodeo, Augmentation of tendon-to-bone healing, *J. Bone Joint Surg.*, 2014, **96**, 513–521.

2 C. P. Chiodo, M. Glazebrook, E. M. Bluman, B. E. Cohen, J. E. Femino, E. Giza, W. C. Watters III, M. J. Goldberg, M. Keith and R. H. Haralson III, Diagnosis and treatment of acute achilles tendon rupture, *J. Am. Acad. Orthop. Surg.*, 2010, **18**, 503–510.

3 C. D. Smith, S. Alexander, A. M. Hill, P. E. Huijsmans, A. M. Bull, A. A. Amis, J. F. De Beer and A. L. Wallace, A biomechanical comparison of single and double-row fixation in arthroscopic rotator cuff repair, *J. Bone Joint Surg.*, 2006, **88**, 2425–2431.

4 M. A. Zumstein, B. Jost, J. Hempel, J. Hodler and C. Gerber, The clinical and structural long-term results of open repair of massive tears of the rotator cuff, *J. Bone Joint Surg. Am. vol.*, 2008, **90**, 2423–2431.

5 S. K. M. Perikamana, J. Lee, T. Ahmad, E. M. Kim, H. Byun, S. Lee and H. Shin, Harnessing biochemical and structural cues for tenogenic differentiation of adipose derived stem cells (adscs) and development of an in vitro tissue interface mimicking tendon-bone insertion graft, *Biomaterials*, 2018, **165**, 79–93.

6 S. Patel, J. M. Caldwell, S. B. Doty, W. N. Levine, S. Rodeo, L. J. Soslowsky, S. Thomopoulos and H. H. Lu, Integrating soft and hard tissues via interface tissue engineering, *J. Orthop. Res.*, 2018, **36**(4), 1069–1077.

7 L. A. Kuntz, L. Rossetti, E. Kunold, A. Schmitt, R. von Eisenhart-Rothe, A. R. Bausch and R. H. Burgkart, Biomarkers for tissue engineering of the tendon-bone interface, *PLoS One*, 2018, **13**, e0189668.

8 C. Zhu, S. Pongkitwitoon, J. Qiu, S. Thomopoulos and Y. Xia, Design and fabrication of a hierarchically structured scaffold for tendon-to-bone repair, *Adv. Mater.*, 2018, **30**(16), 1707306.

9 D. W. Youngstrom and J. G. Barrett, Engineering tendon: Scaffolds, bioreactors, and models of regeneration, *Stem Cells Int.*, 2015, **2016**, 3919030.

10 D. Rana, H. Zreiqat, N. Benkirane-Jessel, S. Ramakrishna, M. Ramalingam and R. Medicine, Development of decellularized scaffolds for stem cell-driven tissue engineering, *J. Tissue Eng. Regener. Med.*, 2017, **11**, 942–965.

11 F. Pati, J. Jang, D. H. Ha, S. W. Kim, J. W. Rhie, J. H. Shim, D. H. Kim and D.-W. Cho, Printing three-dimensional tissue analogues with decellularized extracellular matrix bioink, *Nat. Commun.*, 2014, **2**, 3935.

12 A. Shpichka, A. Koroleva, D. Kuznetsova, R. I. Dmitriev and P. Timashev, Multi-Parametric Live Cell Microscopy of 3D Tissue Models, in *Advances in Experimental Medicine and Biology*, 2017, vol. 1035, pp. 71–81.

13 D. Wang, X. Jiang, A. Lu, M. Tu, W. Huang and P. Huang, Bmp14 induces tenogenic differentiation of bone marrow mesenchymal stem cells in vitro, *Exp. Ther. Med.*, 2018, **16**, 1165–1174.

14 J. Cai, Y. Yang, C. Ai, W. Jin, D. Sheng, J. Chen and S. Chen, Bone marrow stem cells-seeded polyethylene terephthalate

scaffold in repair and regeneration of rabbit achilles tendon, *Artif. Organs*, 2018, **42**, 1086–1094.

15 J. Peng, L. Chen, K. Peng, X. Chen, J. Wu, Z. He and Z. Xiang, Bone marrow mesenchymal stem cells and endothelial progenitor cells co-culture enhances large segment bone defect repair, *J. Biomed. Nanotechnol.*, 2019, **15**, 742–755.

16 L. Chen, J. Wu, C. Wu, F. Xing, L. Li, Z. He, K. Peng and Z. Xiang, Three-dimensional co-culture of peripheral blood-derived mesenchymal stem cells and endothelial progenitor cells for bone regeneration, *J. Biomed. Nanotechnol.*, 2019, **15**, 248–260.

17 B. Walia and A. H. Huang, Tendon stem progenitor cells: Understanding the biology to inform therapeutic strategies for tendon repair, *J. Orthop. Res.*, 2018, DOI: 10.1002/jor.24156.

18 T. Wu, Y. Liu, B. Wang, Y. Sun, J. Xu, L. W. Yuk-Wai, L. Xu, J. Zhang and G. Li, The use of cocultured mesenchymal stem cells with tendon-derived stem cells as a better cell source for tendon repair, *Tissue Eng. Part A*, 2016, **22**, 1229–1240.

19 I. Calejo, R. Costa-Almeida, A. I. Goncalves, D. Berdecka, R. L. Reis and M. E. Gomes, Bi-directional modulation of cellular interactions in an *in vitro* co-culture model of tendon-to-bone interface, *Cell Prolif.*, 2018, e12493.

20 E. D. Silva, P. S. Babo, R. Costa-Almeida, R. M. A. Domingues, B. B. Mendes, E. Paz, P. Freitas, M. T. Rodrigues, P. L. Granja and M. E. Gomes, Multifunctional magnetic-responsive hydrogels to engineer tendon-to-bone interface, *Nanomedicine*, 2018, **14**, 2375–2385.

21 C. Zhang, Q. Li, S. Deng, W. Fu, X. Tang, G. Chen, T. Qin and J. Li, Bfgf- and capp-loaded fibrin clots enhance the bioactivity of the tendon-bone interface to augment healing, *Am. J. Sports Med.*, 2016, **44**, 1972–1982.

22 J. Cai, J. Wang, K. Ye, D. Li, C. Ai, D. Sheng, W. Jin, X. Liu, Y. Zhi, J. Jiang, *et al.* Dual-layer aligned-random nanofibrous scaffolds for improving gradient microstructure of tendon-to-bone healing in a rabbit extra-articular model, *Int. J. Nanomed.*, 2018, **13**, 3481–3492.

23 M. Yang, J. Yang, C.-W. Li and J. L. Zhao, Generation of concentration gradient by controlled flow distribution and diffusive mixing in a microfluidic chip, *Lab-on-a-Chip*, 2002, **2**, 158–163.

24 K. Deekshith, J. Sameer and P. P. Intensification, Design and optimization of microfluidic device for generating robust uniform concentration gradients, *Chem. Eng. Process.*, 2018, **124**, 155–163.

25 F. Zheng, Z. Pu, E. He, J. Huang, B. Yu, D. Li and Z. H. Li, From functional structure to packaging: Full-printing fabrication of a microfluidic chip, *Lab-on-a-Chip*, 2018, **18**, 1859–1866.

26 L. J. Ning, Y. J. Zhang, Y. Zhang, Q. Qing, Y. L. Jiang, J. L. Yang, J. C. Luo and T. W. Qin, The utilization of decellularized tendon slices to provide an inductive microenvironment for the proliferation and tenogenic differentiation of stem cells, *Biomaterials*, 2015, **52**, 539–550.

27 S. W. Chung, H. Park, J. Kwon, G. Y. Choe, S. H. Kim and J. H. Oh, Effect of hypercholesterolemia on fatty infiltration and quality of tendon-to-bone healing in a rabbit model of a chronic rotator cuff tear: Electrophysiological, biomechanical, and histological analyses, *Am. J. Sports Med.*, 2016, **44**, 1153–1164.

28 F. Kurth, K. Eyer, A. Franco-Obregón and P. S. Dittrich, A new mechanobiological era: Microfluidic pathways to apply and sense forces on cells, *Curr. Opin. Chem. Biol.*, 2012, **16**, 1.

29 R. H. Lam, Y. Sun, W. Chen and J. Fu, Elastomeric microposts integrated into microfluidics for flow-mediated endothelial mechanotransduction analysis, *Lab Chip*, 2012, **12**, 1865–1873.

30 X. Li, J. Xie, J. Lipner, X. Yuan, S. Thomopoulos and Y. Xia, Nanofiber scaffolds with gradations in mineral content for mimicking the tendon-to-bone insertion site, *Nano Lett.*, 2009, **9**, 2763–2768.

31 S. Park, J. W. Choi and Y. K. Kim, Microfluidic chip for the detection of biological toxic effects of polychlorinated biphenyls on neuronal cells, *J. Biomed. Nanotechnol.*, 2013, **9**, 880–885.

32 S. H. Jeon, K. H. Hwang, W. S. Jung, H. J. Seo, S. W. Nam, J. H. Boo and S. H. Yun, Flow manipulation in thread-based microfluidics by tuning the wettability of wool, *J. Biomed. Nanotechnol.*, 2015, **11**, 319–324.

33 S. Yi, F. Ding, L. Gong and X. Gu, Extracellular matrix scaffolds for tissue engineering and regenerative medicine, *Curr. Stem Cell Res. Ther.*, 2017, **12**, 233–246.

34 C. Zhu, S. Pongkitwitoon, J. Qiu, S. Thomopoulos and Y. Xia, Design and fabrication of a hierarchically structured scaffold for tendon-to-bone repair, *Adv. Mater.*, 2018, **30**, e1707306.

35 J. K. Lim, J. Hui, L. Li, A. Thambyah, J. Goh and E. H. Lee, Enhancement of tendon graft osteointegration using mesenchymal stem cells in a rabbit model of anterior cruciate ligament reconstruction, *Arthroscopy*, 2004, **20**, 899–910.

36 H. W. Ouyang, J. C. Goh and E. H. Lee, Use of bone marrow stromal cells for tendon graft-to-bone healing: Histological and immunohistochemical studies in a rabbit model, *Am. J. Sports Med.*, 2004, **32**, 321–327.

37 L. V. Gulotta, D. Kovacevic, S. Montgomery, J. R. Ehteshami, J. D. Packer and S. A. Rodeo, Stem cells genetically modified with the developmental gene mt1-mmp improve regeneration of the supraspinatus tendon-to-bone insertion site, *Am. J. Sports Med.*, 2010, **38**, 1429–1437.

38 G. Verdiyeva, K. Koshy, N. Glibbery, H. Mann and A. M. Seifalian, Tendon reconstruction with tissue engineering approach–a review, *J. Biomed. Nanotechnol.*, 2015, **11**, 1495–1523.

39 L. Chen, C. Jiang, S. R. Tiwari, A. Shrestha, P. Xu, W. Liang, Y. Sun, S. He and B. Cheng, Tgif1 gene silencing in tendon-

derived stem cells improves the tendon-to-bone insertion site regeneration, *Cell. Physiol. Biochem.*, 2015, **37**, 2101–2114.

40 M. Ni, P. P. Lui, Y. F. Rui, Y. W. Lee, Y. W. Lee, Q. Tan, Y. M. Wong, S. K. Kong, P. M. Lau, G. Li, *et al.* Tendon-derived stem cells (tdscs) promote tendon repair in a rat patellar tendon window defect model, *J. Orthop. Res.*, 2012, **30**, 613–619.

41 H. Song, Z. Yin, T. Wu, Y. Li, X. Luo, M. Xu, L. Duan and J. Li, Enhanced effect of tendon stem/progenitor cells combined with tendon-derived decellularized extracellular matrix on tendon regeneration, *Cell Transplant.*, 2018, **1**, 1–10.